Least-Squares Migration in the Image Domain with Sparsity Constraints: An Approach for Super-Resolution in Depth Imaging

Bruno Pereira-Dias(*), André Bulcão, Djalma Manoel Soares Filho , Luiz Alberto Santos, Roberto de Melo Dias – PETROBRAS; Felipe Prado Loureiro, Felipe de Souza Duarte – Fundação Gorceix

Abstract

In this work we present an application of the least-squares migration in the Image Domain with sparsity constraints. It is known that linear algorithms based on L_2-norm improve the image resolution, altough restricted to the original bandwidth of the seismic data. On the other hand, non-linear algorithms (based on convex optimization) with sparsity constraint are able to extend the image spectral bandwidth resulting in a super-resolution depth-imaging technique even if provided with incomplete measurements. We give an overview of the mathematical formulation and show a numerical application on a synthetic model showing significant correction on the migration amplitude and impressive gain in resolution when compared to the conventional migration algorithm.

Introduction

One of the earliest applications of least-squares migration was realized by Nemeth, Wu and Schuster, 1999, in the data domain. Later, Hu, Schuster and Vasalek (2001) worked out the least-squares migration in the image domain, but naming it as migration deconvolution. In their work, they interpreted the Hessian with the concept of the Point Spread Function, ubiquitously used in the image processing, medical imaging and astronomy community to retrieve images with higher resolution (see **Figure 1**). However, only recently least-squares migration has been applied in large size 3D imaging projects (Fletcher et al., 2012 and Letki et al. 2015).

The power behind least-squares migration comes from a different mind-set which was envisioned by Albert Tarantola more than 30 years ago: "Imaging will not be based on principles, but on well-posed questions about the properties of the Earth's interior" (Tarantola, 1986). Understanding the migration problem as an inversion problem allows not only for correcting the migration amplitudes even on geologically complex models, but to drastically increase the image resolution.

To achieve this goal, this work combines the least-squares migration in the Image Domain, using the concept of Point Spread Function, with the profound ideas of the vibrant area of compressive sensing and sparse recovery, to achieve super-resolution in depth imaging.

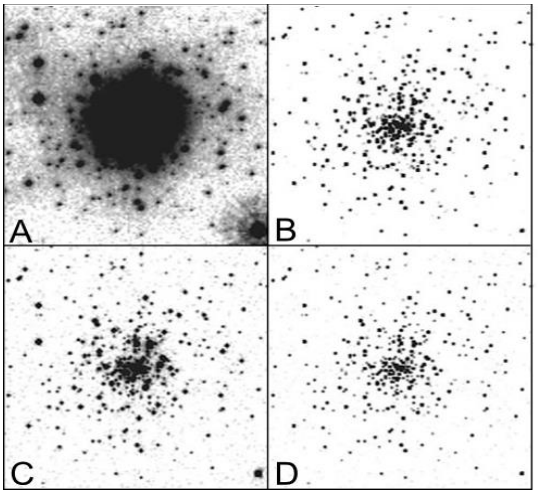

Figure 1: (A) An original Hubble image with the flawed mirror. (B) Image with PSF processing. (C) Image after Hubble's lens correction. (D) Image after lens correction and PSF processing. Note that the PSF processed image (B) has resolution equivalent to the image after the lens correction (C), but it is further enhanced with the PSF processing (D). [Figure adapted from Jansson, P. A., 1997]

To grasp the essence of the interesting results achieved by the compressive sensing community, we present on **Figure 2 (left)** the matrix completion problem. It consists of filling in the missing entries of a partially observed matrix, X, which seems like to be an unsolvable problem. However, with some underlying hypothesis such as low-rank, there are theorems that prove that such matrices can be, in most cases, filled exactly (Candès and Recht, 2009). An example of application is the Netflix problem, in which the presented matrix is partially filled with customers' evaluation of movies. For this problem, the low-rank hypothesis is reasonable since many people share the same taste in movies, providing an underlying structure to the matrix. Netflix awarded researchers the amount of $1M for solving this problem (Netflix, 1997-2009). More examples and applications of signal and image recovery from highly incomplete data can be found in (Candès and Romberg, 2005).

Of greater concern to this work, is a related problem – the spectral completion problem (**Figure 2 (right)**), which consists of filling the amplitude spectrum of seismic image even with incomplete and bandlimited observed data. This work shows, using a synthetic example, that least-squares migration with sparsity hypothesis utilizing techniques of convex optimization is able to provide a super-resolution image in depth, recovering most of the original reflectivity, extending its original spectrum bandwidth and correcting the depth amplitudes.

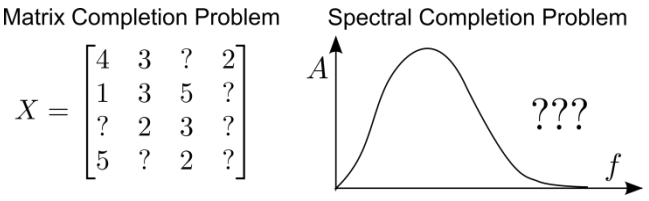

Figure 2: (left) The matrix completion problem is the task of filling in the missing entries of a partially observed matrix, X. (right) The spectral completion problem is the task of filling the unrecorded amplitude spectrum of observed data. Both are ill-posed problems unless underlying hypothesis or constraints are added.

Least-squares migration

The least-squares migration may be formulated as an inversion problem in which the objective is to find the reflectivity (or the image), $\boldsymbol{r}$, which best explains the observed data according to a least squares objective function $E(\boldsymbol{r})$:

$$\boldsymbol{r} = argmin\, E(\boldsymbol{r}) = \frac{\mathbf{1}}{\mathbf{2}}\|\boldsymbol{u}(\boldsymbol{r}) - \boldsymbol{d}\|^{\mathbf{2}} \quad (1)$$

where $\boldsymbol{u}$ is the synthetic data modeled by a linear equation (Born modeling) and $\boldsymbol{d}$ is the observed data. The least squares solution of equation (1) is:

$$\boldsymbol{H}\boldsymbol{r} = -\boldsymbol{\nabla}\boldsymbol{E}\ , \quad (2)$$

that is mathematically (but not numerically) equivalent to

$$\boldsymbol{r} = -\boldsymbol{H}^{-\mathbf{1}}\boldsymbol{\nabla}\boldsymbol{E}\ . \quad (3)$$

It is possible to deduce that $\boldsymbol{\nabla}\boldsymbol{E} = \boldsymbol{J}^{\boldsymbol{T}}\boldsymbol{d} = \boldsymbol{m}$ corresponds to the traditional migration. $\boldsymbol{J}^{\boldsymbol{T}}$ is the adjoint of the Born modeling operator $\boldsymbol{J}$ and $\boldsymbol{H} = \boldsymbol{J}^{\boldsymbol{T}}\boldsymbol{J}$ is called the Hessian which is the second derivatives of $E(\boldsymbol{r})$.

The remarkable difference between the traditional migration and the least squares migration is the presence of the Hessian $\boldsymbol{H}$. It is known that the Hessian is a spatially variant operator which encodes:

- Illumination from the source and the receiver wavefield.
- Resolution associated with the band limited nature of the seismic signal.
- Wavelet signature employed on the migration and modeling.

One concludes, therefore, that neglecting these effects (which is often done in traditional imaging schemes) plagues the final quality and reliability of the seismic images delivered to the interpreters.

On the other hand, the explicit computation and the storage of the Hessian (as a matrix, for example) is computationally infeasible, since the number of its elements is the square of the number of parameters in the model (i. e., $(N_x N_y N_z)^2$ where N_i is the number of grid points in the direction i). This is the reason why it is imperative to interpret the Hessian as an operator. The approach to solve equation (2) distinguishes the application domain of the least-squares migration (Fletcher et al, 2016). A summarized comparison of the algorithms is given in Table 1.

- **Data domain**: From the interpretation that $\boldsymbol{H} = \boldsymbol{J}^{\boldsymbol{T}}\boldsymbol{J}$, one solves the problem of Equation (1) by using the Born modeling (encoded in the operator $\boldsymbol{J}$) and by the migration operator $\boldsymbol{J}^{\boldsymbol{T}}$. In this formulation, the objective function is done by a comparison between modeled and procecessed field data, that is, in the data domain. The gradient of this objective function corresponds to the migration of the data residual. Usually, the model is updated following a steepest descent or pre-conditioned conjugate gradient scheme (Dai et. al, 2012). If no blending or decimation strategy is employed, each iteration of this algorithm has the computational cost of a direct modeling of the dataset and a traditional migration.

- **Image domain**: The image-domain least-squares migration also comes from the interpretation that $\boldsymbol{H} = \boldsymbol{J}^{\boldsymbol{T}}\boldsymbol{J}$. But, on this formulation, one evaluates the Hessian in predefined points of the model by the Born modeling of unit scattering followed by a traditional migration. The outputs of this scheme are the so called Point Spread Functions (PSFs), which describe the response of an imaging system to a point reflectivity. More importantly, the PSFs explicitly encode the illumination and blurring effects present in the seismic imaging process. The computational cost to obtain one grid of PSFs is equal to a direct modeling and a traditional migration. After the retrieval of the Hessian in the specific points, one can utilize the operator $\boldsymbol{H}$ as a multidimensional spatially variant convolution-like operator and implement an iterative optimization algorithm to reduce the difference between $\boldsymbol{H}\boldsymbol{r}$ and $\boldsymbol{m}$. This comparison is realized in the image domain and it is a post-migration operation, which can be done on pre- or post-stacked image gathers.

In this work, we utilize the image domain formulation, but one should be aware that the sparsity constraint can be applied in both formulations.

Table 1: Comparison of the distinct approaches for least-squares migration $\boldsymbol{d}$ is the observed data, $\boldsymbol{J}$ is the linearized modeling operator (Born modeling), $\boldsymbol{r}$ is the reflectivity and and $\boldsymbol{m}$ is the traditional migration.

Born Mod.	Trad. Migr.	LSM Data Domain	LSM Image Domain
$\boldsymbol{u} = \boldsymbol{J}\boldsymbol{r}$	$\boldsymbol{m} = \boldsymbol{J}^{\boldsymbol{T}}\boldsymbol{d}$	$\boldsymbol{r} = [\boldsymbol{J}^{\boldsymbol{T}}\boldsymbol{J}]^{-\mathbf{1}}\boldsymbol{J}^{\boldsymbol{T}}\boldsymbol{d}$	$\boldsymbol{r} = [\boldsymbol{J}^{\boldsymbol{T}}\boldsymbol{J}]^{-\mathbf{1}}\boldsymbol{m}$

Figure 3 indicates what is necessary for the evaluations of the Point Spread Function: (1) to choose a number of unit scattering grids, which should be the most compact possible but without the interference from neighboring the Point Spread Functions, (2) estimation of the source signature (wavelet) and (3) a velocity model for the Born modeling and migration. Also, the geometry of acquisition should be provided in order to model the migration response for the acquired dataset.

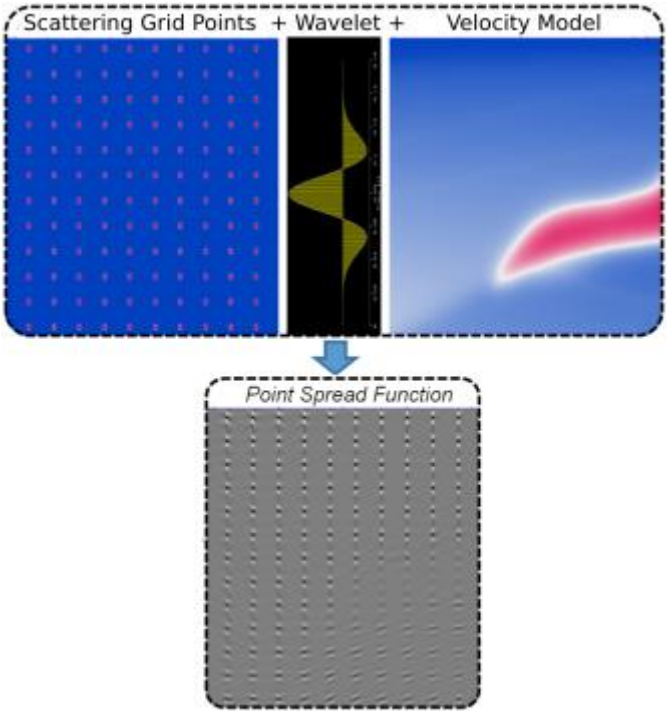

Figure 3: Scattering grid points, wavelet and velocity model (top) are necessary to estimate the Point Spread Functions by wavefield modeling. One can observe the distortion on the deepest Point Spread Functions due to the velocity model variations.

Sparsity Constraint

A traditional approach for least-squares migration in the Image Domain is to consider the L_2-norm objective function (Valenciano et al., 2009), aiming to retrieve the reflectity $\boldsymbol{r}$, such that,

$$\boldsymbol{r} = argmin\ E(\boldsymbol{r}) = \frac{1}{2}\left\| C_d^{-\frac{1}{2}}[\boldsymbol{H}r - m]\right\|^2. \qquad (4)$$

That is, $\boldsymbol{r}$ is the reflectivity which minimizes the L_2-norm of the difference between the migrated image, m, and the reflectivity response to the Hessian or its approximation using the Point Spread Functions. The term $C_d^{-1/2}$ is a preconditioner to the inversion problem, and one popular choice is to use the pseudo-Hessian (Shin et. al, 2001), which corresponds to the compensation for the illumination by the source wavefield.

A computationally affordable solution to the problem (4) is to apply an iterative algorithm, such as the steepest-descent scheme:

$$r_{n+1} = r_n - \alpha C_d^{-1}\boldsymbol{H}^{\boldsymbol{T}}(\boldsymbol{H}r_n - m)\ , \qquad (5)$$

where n is the iteration number and α is the scale-factor. It is known that linear iterative algorithms based on L_2-norm improve the image resolution and corrects for illumination effects, but the bandwidth of the outcome is restricted same as the input seismic image (Rosa, 2010).

o further increase the image resolution, one may impose a sparsity constraint. As explained in **Figure 4**, applying an L_1-norm regularization is a known technique to sparsify the solution of an inverse problem (Candès and Romberg, 2005). One way to do it is by adding a regularization term to the objective function (Fletcher, 2012):

$$\boldsymbol{r} = argmin\ E(\boldsymbol{r}) = \frac{1}{2}\left\| C_d^{-\frac{1}{2}}[\boldsymbol{H}r - m]\right\|^2 + \frac{\lambda}{p}|\boldsymbol{r}|_p \qquad (6)$$

where $|\boldsymbol{r}|_p$ is the L_p-norm of the reflectivity. However, there are some practical issues with this approach. The L_p-norm is not differentiable for $p \leq 1$, so in practice it needs an stabilization factor. Furthermore, the estimating the regularization factor λ is not intuitive and usually requires exhaustive testing and it is hard to generalize for different applications.

A preferred approach is the penalty method (Peters & Herrmann, 2017), in which the problem (**6**) is restated as

$$\boldsymbol{r} = argminE(\boldsymbol{r}) = \frac{1}{2}\left\| C_d^{-\frac{1}{2}}[\boldsymbol{H}r - m]\right\|^2 \ such\ that\ |\boldsymbol{r}|_p < \tau. \qquad (7)$$

In the case of the L_1-norm, the iterative solution of problem **(7)** can be implemented by the successive application of the soft-thresholding operation (Donoho and Jonhstone, 1994) (which diminishes the L_1-norm) at the update direction (which decreases the L_2-norm):

$$r_{n+1} = S_\tau\left(r_n - \alpha\boldsymbol{H}^{\boldsymbol{T}}(\boldsymbol{H}r_n - m)\right) \qquad (8)$$

in which S_τ is the point-wise operation defined as

$$S_\tau(r) = \begin{cases} r + \tau, & if\ \ r < -\tau \\ 0, & if\ \ |r| \leq \tau \\ r - \tau, & if\ \ r > \tau \end{cases}. \qquad (9)$$

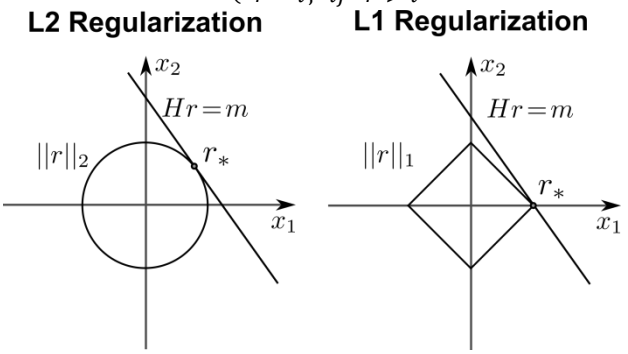

Figure 4: Schematic comparison of L_1 and L_2 regularization. The solution of the least-squares migration problem, r_*, in the intersection of the hyperplane $\boldsymbol{H}r = m$ and the L_p-ball $\|\boldsymbol{r}\|_p$ for $p = 1\ or\ 2$. L_2 regularization provides a minimum distance solution, but not a sparse solution since the components favors to be non-zero. Since the L_1-ball is diamond shaped the solution to this problem usually falls on one of the edges, where most of

the components of the solution vanishes. [Figure adapted from (Tibshirani, 1996)].

Numerical Application

A numerical application of the least-squares migration with sparsity constraint is realized on a synthetic model with the dimensions and characteristics of some regions of the pre-salt area of the Santos Basin, in Brazil, shown in **Figure 5**. We put a reference horizontal reflector, with constant reflectivity, to the reflectivity model, at the depth of 7km for analysis of the resolution and illumination effects. The dataset utilized for this numerical application was generated with Born modeling, which ensures that no (internal) multiples are generated from the reflectivity model. For the data modeling, it was used a towed-streamer geometry of acquisition with receiver cables of 6 km offset and the source signature utilized was a Ricker wavelet with 45 Hz cut frequency.

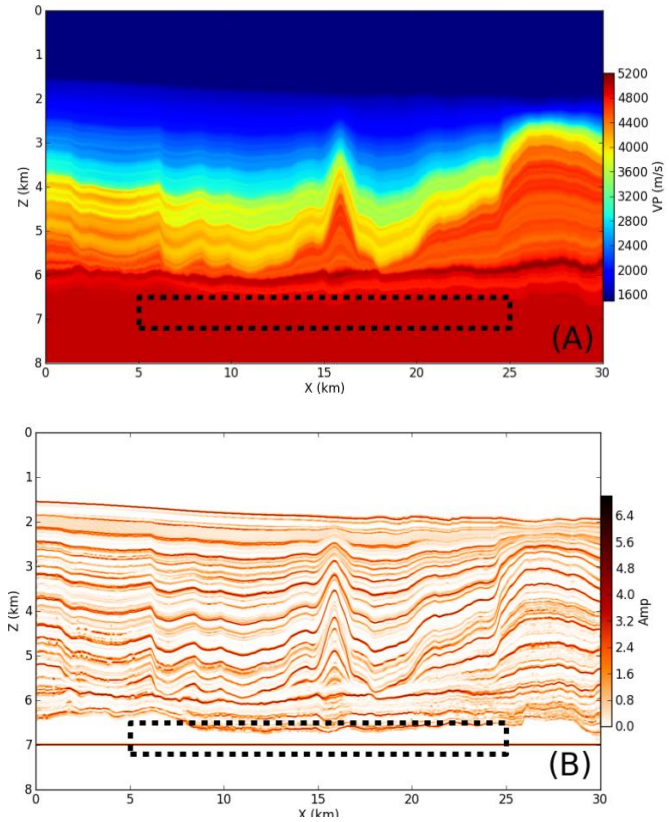

Figure 5: Synthetic model for the application of the LSM (A) The velocity model for the evaluation of the Point Spread Functions (modeling and migration). (B) Reference reflectivity model. Observe that at 7 km depth there is a reference constant reflector. The dashed black region corresponds to the zoomed region correspondent to Figure 6.

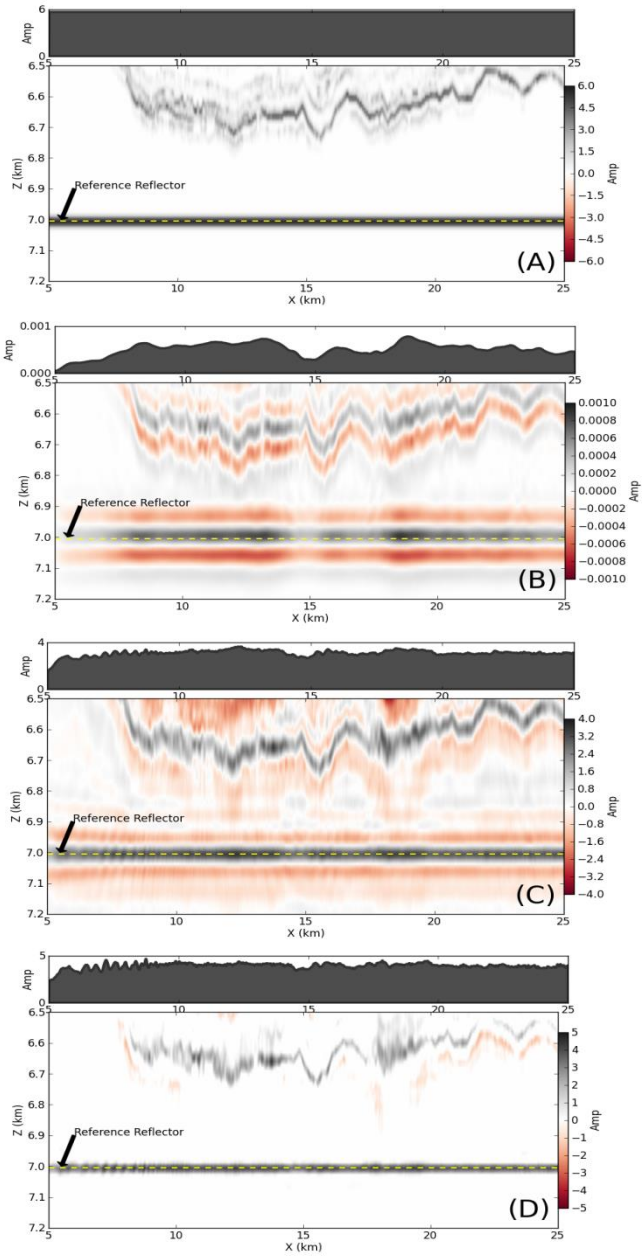

Figure 6: Application of least-squares migration in the Image Domain for the outlined region of the synthetic model of Figure 5. (A) Reference reflectivity. (B) Traditional RTM (C) Least-squares migration with L_2-norm. (D) Least-squares migration with sparsity constraint (L_1-norm). On the top of each figure it is displayed the amplitude extracted on the reference reflector. One should note the variation of amplitude observed in the traditional migration (B), which is significantly reduced in the least-squares migration (C) and (D). Also, it is visible the considerable gain in resolution using sparsity constraint comparing (C) to (D).

The results of the application of the least-squares migration are displayed in **Figure 6**, which shows only the region of interest. Comparing the correct reflectivity (**Figure 6A**) with the result of traditional Reverse Time Migration (RTM) (**Figure 6B**) one realizes how significant the illumination effect is, which can be seen by the amplitude extracted at the depth of the reference reflector. It is also striking the loss of resolution on the image. The result of least-squares migration with L_2-norm (**Figure 6C**) improves the image resolution by reducing the side-lobes of the image in the reference reflector depth and greatly corrects for the amplitude effects. Even greater resolution gain is seen in the least-squares migration with L_1 constraint (**Figure 6D**), in which the reference reflector is mostly recovered and the image is much sharper. **Figure 7** contains the normalized spectrum of the images shown in **Figure 6**, which reinforces the previous statements: (1) The spectrum is broadened with the least-squares migration with L_2-norm iterative algorithm, but restricted to the bandwidth of the RTM image. (2) The recovery of the image's spectrum in the higher wavenumbers is only achieved by the least-squares migration with L_1 constraint.

We emphasize that this gain in resolution with illumination correction could not be done with a simple trace-by-trace approach since the lateral and depth wavefield illumination and resolution should be taken into account. Also, the non-stationary property of the Point Spread Functions are a needful requisite to the modelling stage, thus allowing to remove the illumination effects and correctly restore the reflectivity.

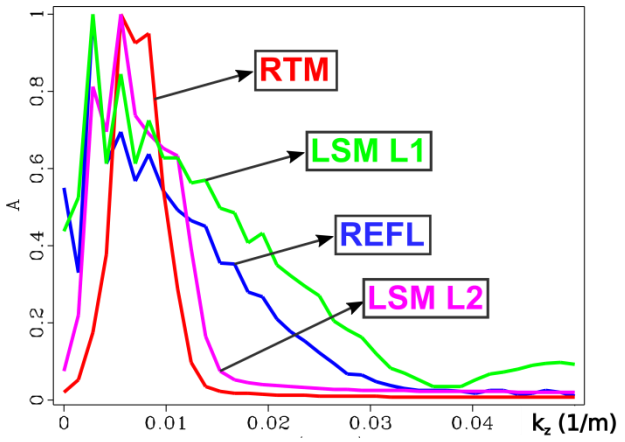

Figure 7: Normalized mean vertical spectra of the images shown in **Figure 6**. Note that the traditional RTM consists a bandlimited image, whose its spectrum is broadened by least-squares migration with L_2-norm, restricted to the original bandwidth of the input. However, only the least-squares migration with sparsity constraint (L_1-norm) can fill the wavelengths closer to the true reflectivity.

Discussion

The application of the sparsity constraint for least-squares migration with real data is more challenging, since noise is present and usually viscoelastic effects are not accounted for the retrieval of the Point Spread Functions, due increase in computational cost or difficulty on obtaining the viscoelastic parameters. Migration defocusing may also happen due to incorrect migration velocity model. Such an error will not be corrected by the least-squares migration. Therefore, some practical considerations are helpful in such applications:

- **Warm-start with L2 Norm:** Since the sparsity constraint leads to reduction in the image amplitude, it is preferable to apply it after the image is balanced and the side-lobes of the reflection are diminished. Therefore optimization with L_2-norm can be applied as a warm-start and as initial solution for the optimization with the L_1 constraint.

- **Adaptive thresholding:** Warm-starting with the L_2-norm optimization may leave some amplitude unbalance in the image. In this case, adaptive thresholding may be used. For this, the penalty parameter τ is promoted to be a spatially variant function and the thresholding may be defined by a percentage of the root mean square values within some predefined window.

- **Structure-oriented filtering:** The presence of noise or undesired events such as multiples in the migrated image may reduce the quality of the least-squares migration result. In this case, other constraints such as structure-oriented filtering (Hale, 2009) can be imposed and interpreted as an additional geological constraint to inversion problem.

Another improvement to the proposal of this work is to use more sophisticated optimization schemes such as the Gradient Projection for Sparse Reconstruction (GPSR) (Figueiredo et al. 2007), Spectral Projected Gradient - L1 (SPG-L1) (van den Berg and Friedlander, 2008), Sparse Reconstruction by Separable Approximation (SpaRSA) (Wright et al., 2009), among others. Even though these algorithms rely on the basic idea of the iterative shrinkage method, they have specialized line-search recipes and accelerating strategies built-in, which yield more performance in a variety of optimization problems.

It should also be emphasized that L_1 regularization is not restricted to the space domain. Applications on wavelet, curvelet, total variation or other domains can be employed according to each case of interest.

Conclusions

We presented an application of the least-squares migration in the Image Domain with sparsity constraints, resulting in a super-resolution depth-imaging technique even though the input was a bandlimited image plagued with illumination issues. This was made possible by a mathematical formulation with sparsity promotion method. Also, this work shows that the least-squares migration can correct the migration amplitudes even on geologically complex models, thus it should be considered in imaging projects in order to provide the interpreters a more reliable image.

Acknowledgments

The authors would like to thank PETROBRAS for authorizing this publication. Prof. Jessé Costa from Pará Federal University (UFPA) is also acknowledged for helpful discussion related to sparse optimization methods.

References

van den Berg, E. and Friedlander, M. P., 2008. *Probing the Pareto frontier for basis pursuit solutions*: SIAM J. on Scientific Computing, **31**(2):890-912.

Candès, E., Romberg, J. 2005. *L1-Magic: Recovery of Sparse Signals via Convex Programming*: Available in: https://statweb.stanford.edu/~candes/l1magic/

Candès, E.J., Recht, B., 2009. Exact Matrix Completion via Convex Optimization. Foundations Computational Mathematics, **9:**717.

Dai, W., Fowler, P. and Schuster, G. T., 2012, *Multi-source least-squares reverse time migration*.: Geophysical Prospecting, 60: 681–695.

Donoho, D. and Jonhstone, I., 1994. *Ideal spatial adaptation by wavelet shrinkage*. Biometrika, **81**, 425-455.

Figueiredo. M. A. T., Nowak. R. D, Wright S. J., 2007, *Gradient projection for sparse reconstruction: application to compressed sensing and other inverse problems,* IEEE Journal of Selected Topics in Signal Processing: Special Issue on Convex Optimization Methods for Signal Processing, vol. **1**, no. 4, pp. 586-598.

Fletcher, R.P., Archer, S., Nichols, D., Mao, W., 2012, *Inversion after depth imaging*: Expanded Abstracts, SEG 82nd Annual Meeting, Las Vegas.

Fletcher, R.P., Nichols, D., Bloor, R., Coates, R. T., 2016. Least-squares migration – Data domain versus image domain using point spread function. The Leading Edge, February 2016.

Hale, D., 2009*. Structure-oriented smoothing and semblance:* CWP Report 635, 261-270.

Hu, J., Schuster, G. T. and Valasek, P. A., 2001, *Poststack migration deconvolution*: Geophysics, **66**, 939-952.

Jansson, P. A., 1997*, Deconvolution of Images and Spectras*. 2nd Edition. Academic Press Inc.

Letki, L., Tang. J., Inyang, C. Du, X., Fletcher, R. 2015. *Depth domain inversion to improve fidelity of subsalt imaging: a Gulf of Mexico case study*. First Break, **33**, pp. 81-85.

Nemeth, T.,Wu, C., and Schuster, G. T., 1999*, Least-squares migration of incomplete reflection data*: Geophysics, **64**, 208–221.

Netflix, Inc, 1997-2009, *Netflix Prize*: Available at http://www.netflixprize.com/

Peters, B., Herrmann F. J., 2017. *Constraints versus penalties for edge-preserving full-waveform inversion*.The Leading Edge **36**, 1(2017); pp. 94-100.

Rosa, A. L. R. 2010. Análise do Sinal Sísmico: 1 ed. Sociedade Brasileira de Geofísica: Rio de Janeiro, RJ.

Shin, C., Jang, S., Min, D.-J., 2001, "Improved amplitude preservation for prestack depth migration by inverse scattering theory", Geophysical Prospecting, v. 49, pp. 592-606.

Tarantola, A. 1986. *A strategy for nonlinear elastic inversion of seismic reflection data*: Geophysics, **51**, no. 10, pp. 1893-1903.

Tibshirani. R., 1996. *Regression Shrinkage and Selection via the Lasso*. Journal of the Royal Statistical Society, **B58**, no. 1, pp. 267-288.

Valenciano, A. A., Biondi, L. B., Clapp, R. G, 2009. *Imaging by target-oriented wave-equation inversion*: Geophysics, **74**, no. 6, pp. WCA109-WCA120.

Wright, S., Nowak, R., Figueiredo, M., 2009. *Sparse reconstruction by separable approximation*, IEEE Transactions on Signal Processing, vol. **57**, no. 7, pp. 2479-2493.